Physically-Based Distributed Models for Multi-Layer Ceramic Capacitors

C. R. Sullivan
Yuqin Sun

Found in *IEEE Topical Meeting on Electrical Performance of Electronic Packaging,* Oct. 2003, pp. 185–188.

Physically-Based Distributed Models for Multi-Layer Ceramic Capacitors

Charles R. Sullivan and Yuqin Sun
charles.r.sullivan@dartmouth.edu http://power.thayer.dartmouth.edu
8000 Cummings Hall, Dartmouth College, Hanover, NH 03755, USA, Tel. +1-603-646-2851 Fax +1-603-646-3856

Abstract

Measurements show that lumped RLC models for multilayer ceramic capacitors are inadequate. A new transmission-line model offers advantages over previous transmission-line models: a closer fit to measured data, and a physical basis for the model.

I. Introduction

Conventionally, capacitors are modelled as lumped RLC (resistor-inductor-capacitor) networks. The inductance includes inductance of the leads and inductance of the current path through the capacitor itself. When the lead inductance dominates, the lumped model is accurate. However, when the inductances of the paths through the capacitor itself dominate, an accurate model must be based on distributed capacitance and inductance [1], [2], [3], [4], [5]. Leadless surface-mount multilayer ceramic (MLC) chip capacitors are widely used in applications in which high-frequency behavior and accurate models are critical, and, because of their distributed behavior, they exhibit characteristics that are substantially different from those predicted by the RLC model.

Frequently, the interconnect inductance for a capacitor is also significant, and when it dominates, a lumped RLC model for the combination of a capacitor and its interconnect path can be accurate. However, configurations with low interconnect inductance are increasingly common, such as in the careful board layouts needed for power delivery in high-current low-voltage digital systems. Thus, the inductance of the capacitor itself is often important, and a true distributed model is needed.

The most basic distributed model is a simple lossless transmission line. This can lead to qualitatively and quantitatively useful information about capacitor behavior, and it can lead to simple and useful relationships between capacitor geometry and in-circuit performance [4]. However, the assumption of ideal transmission line behavior does not match the lossy behavior of typical practical capacitors. Lossy transmission line models have been developed in [2], [3], [4], [5]. The standard lossy transmission line configuration does not match measurements, and so a different configuration with resistance in series with the incremental capacitance is used [2], [3], [4], [5] rather than the standard configuration in which the resistance is in parallel with the capacitance. This paper will discuss the physical basis for this model, and describe physically-based refinements that can make the model better match the measured results.

II. Lossless Transmission Line Model

Before considering a model for inductive effects in a capacitor, it is important to note that inductance cannot be defined except for a path forming a complete loop [6]. Thus, we must consider the impedance of a closed path including a capacitor. We consider a surface-mount capacitor on a thin two-layer board, with a current path across the top of the board, through the capacitor, down through vias to the bottom of the board, and returning under the capacitor. We define the impedance of the capacitor as the *difference* between the impedance of the complete loop just described and that of the same board with the capacitor replaced by a short[1].

A transmission line model for a capacitor in this configuration may be derived in two different ways. In [1], [4], [5], the individual pairs of plates correspond to the capacitors in the transmission line. The model is a lumped model, but with hundreds of elements, such that a continuous transmission line model is accurate. The inductance is calculated by considering the total inductance at a height x,

$$L = \mu_0 \frac{x\ell}{w} \tag{1}$$

where μ_0 is the permeability of free space, ℓ is the length of the capacitor (parallel to the current path), w is the width (parallel to the board but perpendicular to current flow), and we assume $w >> x$.

Other authors have taken a different approach: The serpentine path defined by the interleaved plates is considered a folded transmission line [3]. It might seem that these two approaches would lead to different models, but, if losses are neglected, the models become identical.

We consider the two defining characteristics of the lossless line to be the characteristic impedance and the round-trip time for a wave travelling up the transmission line and back down. For a particular type of capacitor that has a given voltage rating, dielectric material, dielectric thickness, and plate thickness, we can describe the capacitance in terms of a constant capacitance per unit volume, C_v. Based on the first approach [4], the characteristic impedance can be written

$$Z_0 = \sqrt{\frac{L'}{C'}} = \sqrt{\frac{\mu_0 \ell/w}{C_v w \ell}} = \frac{1}{w}\sqrt{\frac{\mu_0}{C_v}}. \tag{2}$$

This work was supported in part by the United States Department of Energy under grant DE-FC36-01GO1106 and the United States National Science Foundation under grant ECS-9875204

[1]This is equivalent to defining it as the impedance of the same configuration in the limit of zero board thickness and zero resistivity of the conductor on the board.

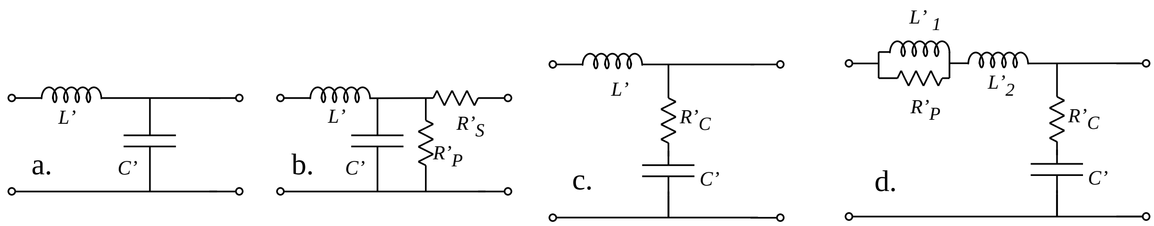

Fig. 1. Incremental sections of four transmission line models. a. Standard lossless. b. Standard lossy. c. A better representation of the origin of dissipation in a capacitor. d. The full model used in Fig. 3.

The round trip time in terms of velocity v is $T = 2h/v$ and can be shown to be [4]:

$$T = 2h\ell\sqrt{\mu_0 C_v}. \tag{3}$$

Alternatively, for the serpentine path model [3], the characteristic impedance is

$$Z_0 = \sqrt{\frac{L'}{C'}} = \frac{h/N}{w}\sqrt{\frac{\mu_0}{\epsilon}}, \tag{4}$$

where N is the number of layers of dielectric, and we neglect the thickness of the plates. The round-trip time is

$$T = 2N\ell\sqrt{\mu_0\epsilon} \tag{5}$$

In terms of the parameters used in this model the capacitance per unit volume can be expressed as

$$C_v = \epsilon\left(\frac{N}{h}\right)^2 \tag{6}$$

If we plug (6) into (2) and (3), we obtain (4) and (5), thus showing that the two models are equivalent if we neglect plate thickness and neglect losses.

III. Measurements

Instruments for impedance measurements fall into two broad categories–impedance analyzers and network analyzers. Network analyzers cover a wide frequency range, but since measurements are referred to a 50 Ω characteristic impedance, they have limited accuracy for the very low impedances that are important in many applications, such as bypass of power busses on high-current digital systems. Impedance analyzers have a more limited frequency range, but are accurate over a wide range of impedance magnitudes, and so are more suitable for our purposes.

For low-impedance measurements, the test fixture design is at least as important as the choice of instrument. Standard test fixtures for impedance measurement of surface-mount components have stray inductance of about 100 nH. Although calibration with a short circuit measurement can subtract this fixture inductance, good results cannot be expected when the quantity being subtracted is two orders of magnitude larger than the circa 1 nH inductance of the capacitors we are measuring. High-performance test-fixtures designed for measuring capacitors with network analyzers are addressed in [7], [8], [9], [3], but these are subject to the limited accuracy at low impedance inherent in the network analyzer approach. To make accurate measurements in a lower impedance range, we used a high performance impedance analyzer (Agilent 4294A) with a new test fixture we developed that has stray inductance under 100 pH, as described in detail in [10].

Although we have measured dozens of MLC capacitors and seen similar characteristics, we focus here on one example that has been modeled in detail: a 100 μF MLC capacitor, rated to have an X5R temperature characteristic. Its dimensions are 6 mm long, 5.3 mm wide, and 2.7 mm high.

IV. Lossy Models

In [3], [5], [4], it is found that, although the standard lossy transmission line model (Fig. 1b) is much better than a simple RLC model, or the lossless line in Fig. 1a, it cannot fit measured data as well as is desired. The model in Fig. 1c), is found to match the data better [3], [4], [5]. This includes time domain tests [4], [5] and frequency-domain tests [3], [5].

The parallel resistance in the standard lossy standard lossy transmission line model (Fig. 1b), R'_P, represents leakage or dielectric loss. Measurements in [5] indicate that both of these effects are unimportant. Based on the first approach to understanding the origin of the transmission line model [4], [5], the series resistance R'_S in this model would represent the resistance of the vertical path along the end metallization on the capacitor, which is very small. Thus, this model should not be expected to work well.

The model in Fig. 1c gives a much better match to measured results [2], [3], [4], [5]. Based on the first approach to understanding the origin of the transmission line model [4], [5], the resistor R'_C models the resistance of the metallization on each plate. Based on the serpentine path model [3], on might naively expect that the series resistance R'_S in Fig. 1b would be a better model for plate resistance. However, in the folded structure, each plate is shared between two transmission line sections, above and below it. Since the plates are very thin, thinner than a skin depth at the frequencies of interest, currents due to wave propagation above and below a plate sum and are both distributed over the entire thickness of the plate. Since the wave propagation is in opposite directions above and below the plate, the net current in the plate is not the current in R'_S in Fig. 1b, but rather is the difference between the current in one section of the model and the next section. This difference in current is precisely the current in R'_C in Fig. 1c. Thus, we once again see that either way of conceptualizing the physical basis for the model leads to the same conclusion.

Another important discrepancy between simple transmission line models and measured characteristics is that the measured characteristics increase in impedance at high frequencies more than the models. This is explained in both [3] and [5] as a result of the dielectric coating over the actual capacitor element. The resulting spacing adds an additional inductance. The tests in [5] partially confirmed that model. We further confirmed the model for the capacitor considered here. The coating is approximately 0.25 mm thick, which, according to (1), introduces 356 pH additional inductance. Our measurements indicate 385 pH additional external inductance, matching to well within the tolerance of our measurement of the coating thickness. We also reduced the coating thickness on one sample by grinding it down by 0.11 mm. This should have reduced inductance by 156 pH; we measured a difference of 169 pH. This confirms the theory, and also indicates that higher performance could be achieved with thinner coatings.

Comparisons of several distributed models to the measured impedance of the 100 μF capacitor are shown in Fig. 2. Fig. 2a shows the performance of the model in Fig. 1c, with additional external inductance modelling the coating thickness. Adjusting the resistance value allows matching the measured depth of the first resonance. However, the remaining higher frequency resonances are still more heavily damped in the measured data than in this model. What is needed is additional frequency-dependent damping.

Although it would be possible to add in additional frequency-dependent damping with no physical motivation in order to make the model fit the data, it is preferable to understand the physical origin of this effect and add the damping appropriately. An additional source of loss, and thus of damping, is eddy-currents in the plates induced by changing magnetic fields. This is similar to ”proximity-effect” in high-frequency magnetic components [11], [12], where it is well-known that a large number of layers—as we have in MLC capacitors—can give rise to substantial proximity effect losses, even when the layers are significantly thinner than a skin depth. In addition, field components perpendicular to planar conductors can induce even greater losses.

A crude model of eddy-current losses in the plates can be obtained by putting a resistor in parallel with the distributed inductance, as shown in Fig. 1d. This results in a loss term that depends upon the square of the voltage across the inductance, which is this also proportional to the square of the derivative of the flux in the inductor, as is appropriate for eddy-current loss. Because only the portion of the flux that goes through the plates, rather than the dielectric, induces losses, the distributed inductance L' is broken into two pieces, L'_1 and L'_2, and the eddy-current loss resistor R'_E is placed in parallel with only one of them. The allocation of total inductance between L'_1 and L'_2 is not critical, but for a given allocation, the value of R'_P is chosen to approximate the experimentally measured damping of secondary resonances. Not shown in Fig. 1 is the external inductance, modelling the thickness of the insulating coating on the capacitor.

The resulting model is compared to experimental data in Fig. 2b, and shows a better, but still imperfect, fit to the data. The

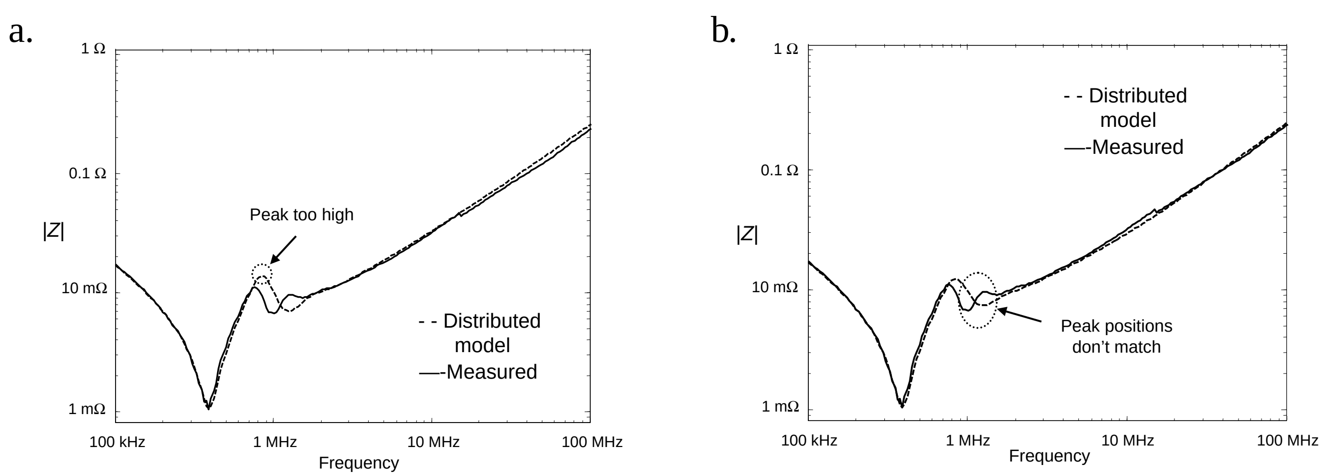

Fig. 2. Simple distributed model for a 100 μF MLC capacitor (a) and intermediate distributed model (b). In the simple model (a), corresponding to Fig. 1c, losses are modeled by series plate resistance. With the resistance chosen to match the resonant frequency as shown, there is not enough damping at higher frequencies. The intermediate model, (b), corresponds to Fig. 1d. It incorporates eddy-current damping as well as plate resistance. Although damping as a function of frequency matches well, the positions of the secondary resonances do not match the data.

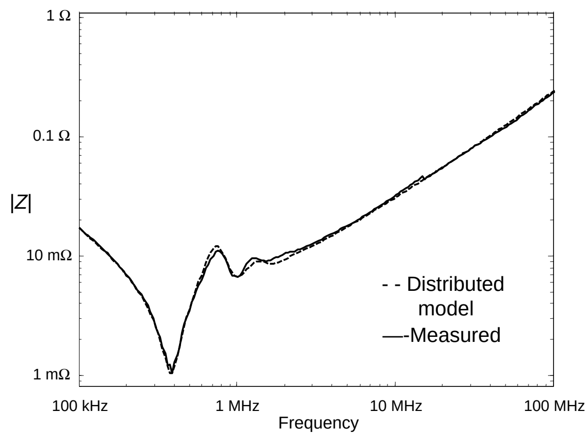

Fig. 3. Final distributed model for a 100 μF MLC capacitor. Incorporates eddy-current damping and plate resistance, and uses non-uniform inductance to match peak positions

most salient discrepancy is that the measured resonant frequencies become slightly more closely spaced at higher frequencies, whereas the model's resonances become slightly more widely spaced. This results in a peak in measured impedance matching up with a dip in modelled impedance at 1.3 MHz—the largest discrepancy between the model and the measurement.

One possible reason for the nonuniform peak spacing is that the accuracy of (1) is reduced when h is not much smaller then w; thus the inductance per unit length is a function of vertical position. Another related effect could be mutual inductance between what we have assumed to be independent inductors. Fig. 3 shows the result of assuming non-uniform inductance over the transmission line, and adjusting parameters to match the experimental data. The model fits the data very well.

V. Conclusion

RLC models for capacitors in packaging with low lead inductance give misleading predictions. The actual high-frequency inductance, determined primarily by lead or packaging inductance, is much smaller than the ESL determined from the first resonant frequency. In the 100 μF capacitor we measured, the high-frequency inductance is smaller by about a factor of five.

A transmission line model is much more accurate. Two different approaches to deriving the model have been compared; both result in quantitatively identical models. Proper placement of damping in the transmission line model is important in order to get good results. Placing distributed resistance in series with the distributed capacitance results in a more accurate model than a standard lossy transmission line with resistance in parallel with the capacitance. Both approaches to deriving the transmission line model are shown to result in this placement of the resistor to model plate resistance. Additional damping at higher frequencies is probably due to eddy current losses and is most appropriately and effectively modeled by distributed resistance in parallel with some of the distributed inductance.

The measured results also show nonuniform spacing of the resonances; this has not been captured by any of the previous models. By adding nonuniform inductance we are able to model this effect accurately.

References

[1] Ch. Joubert, G. Rojat, and A. Beroual, "Magnetic field and current distribution in metallized capacitors", *Journal of Applied Physics*, vol. 76, pp. 5288, 1994.

[2] Larry D. Smith and David Hockanson, "Distributed SPICE circuit model for ceramic capacitors", in *Electronic Components and Technology Conference*, 2001, pp. 523–528.

[3] Larry D. Smith, David Hockanson, and Krina Kothari, "A transmission-line model for ceramic capacitors for cad tools based on measured parameters", in *Electronic Components and Technology Conference*, 2002, pp. 331–336.

[4] A. M. Kern and C. R. Sullivan, "Capacitors with fast current switching require distributed models", in *32nd Annual Power Electronics Specialists Conf.*, 2001.

[5] C.R. Sullivan, Yuqin Sun, and A.M. Kern, "Improved distributed model for capacitors in high-performance packages", in *IEEE Industry Applications Society Annual Meeting*, 2002.

[6] B. H. Evenblij and J. A. Ferreira, "A physical method to incorporate parasitic elements in a circuit simulator based on the partial inductance concept", in *32nd Annual Power Electronics Specialists Conf.*, 2001.

[7] Y. Sakabe, M. Hayashi, T. Ozaki, and J.P. Canner, "High frequency measurement of multilayer ceramic capacitors", *IEEE Transactions on Components, Packaging and Manufacturing Technology, Part B: Advanced Packaging*, vol. 19, pp. 7, 1996.

[8] Y.L. Li, D.G. Figueroa, J.P. Rodriguez, L. Huang, J.C. Liao, M. Taniguchi, J. Canner, and T. Kondo, "A new technique for high frequency characterization of capacitors", in *Proceedings of the 48th Electronic Components and Technology Conference*, 1998, p. 1384.

[9] D.G. Figueroa and Y.L. Li, "A technique for the characterization of multi-terminal capacitors for high frequency applications", in *Proceedings of the 50th Electronic Components and Technology Conference*, 2000, p. 445.

[10] Satish Prabhakaran and Charles R. Sullivan, "Impedance-analyzer measurements of high-frequency power passives techniques for high power and low impedance", in *Conference Record of the 2002 IEEE Industry Applications Conference 37th IAS Annual Meeting*, 2002.

[11] R. W. Erickson and D. Maksimovic, *Fundamentals of Power Electronics*, Kluwer Academic Publishers, second edition, 2001.

[12] E. C. Snelling, *Soft Ferrites, Properties and Applications*, Butterworths, second edition, 1988.